**Biogeosciences
Discussions**

Response of ocean phytoplankton community structure to climate change over the 21st century: partitioning the effects of nutrients, temperature and light

I. Marinov[1], S. C. Doney[2], and I. D. Lima[2]

[1]Department of Earth and Environmental Science, University of Pennsylvania, 240 S. 33rd Street, Hayden Hall 153, Philadelphia, PA 19104, USA
[2]Department of Marine Chemistry and Geochemistry, Woods Hole Oceanographic Institution, 266 Woods Hole Road, Woods Hole, MA 02543, USA

Abstract

The response of ocean phytoplankton community structure to climate change depends upon species competition for nutrients and light, as well as the increase in surface ocean temperature. We propose an analytical framework linking changes in nutrients, temperature and light with changes in phytoplankton growth rates, and we assess our theoretical considerations against model projections (1980–2100) from a global Earth System model. Our proposed "critical nutrient theory" suggests that there is a critical nutrient threshold below (above) which a nutrient change will affect more (less) small phytoplankton biomass than diatom biomass, i.e. the phytoplankton with lower half-saturation coefficient K are influenced more strongly in low nutrient environments. This nutrient threshold broadly corresponds to 45° S and 45° N, poleward of which high vertical mixing and inefficient biology maintain higher surface nutrient concentrations and equatorward of which reduced vertical mixing and more efficient biology maintain lower surface nutrients. In the 45° S–45° N low nutrient region, decreases in limiting nutrients – associated with increased stratification under climate change – are predicted analytically to limit more strongly the net growth of small phytoplankton than the growth of diatoms. In high latitudes, the impact of nutrient decrease on phytoplankton biomass is more significant for diatom biomass than for small phytoplankton biomass, and contributes to diatom declines in the northern marginal sea ice and subpolar biomes. Climate driven increases in surface temperature and changes in light are predicted to have a stronger impact on small phytoplankton than on diatom biomass in all ocean domains. Our analytical predictions explain reasonably well the shifts in community structure under a modeled climate-warming scenario. Further stratification from global warming could result in geographical shifts in the "critical nutrient" threshold and additional changes in ecology.

1 Introduction

Earth system models are emerging with increasing sophistication in, for example, ocean ecology and biogeochemistry, with complex modules incorporating increasing number of plankton groups (e.g., Moore et al., 2002; Aumont et al., 2003; Moore et al., 2004; Lima et al., 2004; Le Quere et al., 2005; Schmittner et al., 2005; Follows et al., 2007) and improvements in the representation of limiting nutrients such as iron (e.g., Moore et al., 2006; Moore and Braucher, 2008). It is therefore important to analyze the basic ecological equations behind these models and offer analytical frameworks for understanding the behavior of such models, including the response to climate change.

Understanding phytoplankton distribution is important, as phytoplankton are responsible for almost half of the total global primary production (Field et al., 1998). Phytoplankton consume inorganic carbon during photosynthesis and are an essential part of the transport of organic carbon from the upper to deep ocean. Diatoms, a phytoplankton group with siliceous tests, are thought to be better at exporting carbon to the deep ocean than nano or picophytoplankton. Coccolithophores, a small phytoplankton with carbonate shells, are responsible for much of the transport of carbonate from the surface ocean to the deep and for associated alkalinity changes. Any future changes in the relative contribution of these phytoplankton types to the total ocean biomass could thus have a significant impact on elemental stoichiometry, ocean biogeochemistry, and ocean carbon storage (e.g., Smetacek, 1999; Falkowski et al., 2004; Cermeno et al., 2008), as well as higher trophic levels that are dependent on them (Falkowski et al., 1998, etc.). Such ecological processes are poorly understood, and have only recently been incorporated in global climate models.

Predicting the response of phytoplankton community structure to climate change is complicated by the fact that phytoplankton growth depends on temperature and competition for light and nutrients, all of which change as the climate warms. While the overall effects of climate change on the biomass of phytoplankton has been addressed in recent studies (Boyd and Doney, 2002; Le Quere et al., 2003; Bopp et al., 2001, 2005),

Phytoplankton response to climate change

I. Marinov et al.

Full Screen / Esc

Printer-friendly Version

Interactive Discussion

none of these studies has analyzed in a theoretical framework the separate impacts of changes in light, nutrients and temperature on the biomass and global distribution of main phytoplankton groups.

At low and mid-latitudes, the effect of reduced upwelling has been argued to result in reduced nutrient supply (and increased light efficiency), with a net negative impact on biomass and marine production (Sarmiento et al., 2004; Steinacher et al., 2010). Using data from an AMT cruise in the Atlantic Ocean, Cermeno et al. (2008) showed larger coccolithophorid-to-diatom biomass and diversity ratios for deeper nutricline depth (i.e., in more stable, less nutrient rich upper-ocean water columns) in the present ocean, and suggested a future transition from diatoms to coccolithophorids following a climate driven stabilization of the water column. These predictions are consistent with a couple of global modeling studies, which have projected a decrease in diatom relative abundance (fraction of diatoms to total biomass) in low and mid-latitudes (Bopp et al., 2005) with climate change, ascribed to decreasing nitrate in the surface layer. In contrast, a longer growing season and decreased ice cover has been suggested to lead to increased marine biomass and thus production at high latitudes (Bopp et al., 2001; Sarmiento et al., 2004; Doney, 2006a; Steinacher et al., 2010).

Here we study the differential impact of climate driven changes in upper ocean nutrients, temperature and light on phytoplankton biomass and community structure. The behavior of the ecological system is based on a set of complex, coupled differential equations describing each of the three phytoplankton types and model nutrients. It is well known that different phytoplankton drawdown nutrients more or less efficiently depending on their half saturation (K) values, with lower K phytoplankton drawing down nutrients more efficiently in the stratified low latitudes. Furthermore, different phytoplankton types have different light requirements, and their response to light will also depend on their chlorophyll to carbon ratio (Chl/C), the initial slope α of the photosynthesis-irradiance (P-I) curve, nutrient concentrations and temperature.

The model of Geider et al. (1998) has become the model of choice for representing phytoplankton growth in the most recent state-of-the-art models (Le Quere et al., 2005;

Moore et al., 2002, 2004). In the framework of this photosynthetic model incorporated in the CCSM3 global climate model, we show analytically and verify in future climate projections that changes in nutrients affect the biomass of small phytoplankton (the phytoplankton with lower K in our model) more (less) strongly than diatom biomass in
5   the low-mid latitudes (high latitudes), with the separation between these two types of biomes determined by a "critical nutrient" value. Furthermore, climate driven increases in temperature and changes in light always preferentially affect small phytoplankton compared to diatoms.

2   Biogeochemistry ecosystem model

10 Our analysis is based on global numerical simulations using the Community Climate System Model version 3 (CCSM3, see Collins et al., 2006a), to which has been added prognostic land and ocean carbon cycle and ecosystem dynamics. We use the low spatial resolution version of the CCSM3 as detailed by Yeager et al. (2006). The CCSM3 atmosphere and land models share the identical grid T31x3, a 96 by 48 spectral dy-
15 namical grid of approximately 3.75° horizontal resolution, and the atmosphere component model (Collins et al., 2006b) has 26 levels in the vertical at this resolution. The land component has been modified from the Community Land Model version 3 (Collins et al., 2006a) to incorporate coupled carbon and nitrogen cycles as well as an improved hydrological scheme, as described in Thornton et al. (2009).
20   The ocean physics component of CCSM3 is the Parallel Ocean Program (POP), a z-level, hydrostatic, primitive equation model (Smith and Gent, 2002; Collins et al., 2006a). The version integrated here has the so-called gx3v5 resolution, i.e., 3.6° in longitude, 0.8° to 1.8° in latitude (finer resolution near the equator), and 25 vertical levels with level thickness monotonically increasing from approximately 12 to 450 m (Yeager
25 et al., 2006). The ocean model uses the Gent and McWilliams (1990) parameterization of mesoscale eddy transport effects and (in the vertical) the Large et al. (1994) K-profile parameterization of surface boundary-layer dynamics and interior diapycnal mixing.

Phytoplankton response to climate change

I. Marinov et al.

Title Page

Abstract	Introduction
Conclusions	References
Tables	Figures

◀◀   ▶▶

◀   ▶

Back   Close

Full Screen / Esc

Printer-friendly Version

Interactive Discussion

The biogeochemistry-ecosystem-circulation ocean model (BEC) model consists of upper ocean ecological (Moore et al., 2002, 2004) and full-depth biogeochemical (Doney et al., 2006b) modules embedded in the global 3-D POP ocean general circulation model. The biogeochemistry module follows Doney et al. (2006b) and is an expanded version of the Ocean Carbon Model Intercomparison Project (OCMIP) biotic model (Najjar et al., 2007). This model includes a carbonate chemistry module, which dynamically calculates surface $p\mathrm{CO}_2$ from simulated temperature, salinity, dissolved inorganic carbon and total alkalinity, as well as air-sea gas exchange for CO_2 and O_2. A dynamical iron cycle is incorporated with seasonally-varying atmospheric dust deposition, water-column scavenging and continental sediment source using the parameterizations in Moore et al. (2008). The absorption of shortwave radiation depends on the simulated chlorophyll distribution, thus allowing for biological feedbacks in ocean physics.

The following phytoplankton groups are represented: small phytoplankton class (which incorporates nano/picoplankton and coccolithophores), nitrogen-fixing diazotrophs, and diatoms. A single zooplankton class grazes differentially on the phytoplankton groups. Additional prognostic variables include suspended and sinking particulate matter, DIC (dissolved inorganic carbon), Alk (alkalinity), O_2 (oxygen) and dissolved nutrients: NH_4 (ammonia), NO_3 (nitrate), PO_4 (phosphate), SiO_3 (silicate) and Fe (iron). The model fixes the phytoplankton C/N/P ratios but allows for variations in Fe/C, Si/C and Chl/C ratios depending on ambient nutrient and light availability. The parameterization of nitrogen fixation follows Moore et al. (2006). A thorough validation of ocean-only simulations was recently performed by comparing with a host of observables (Doney et al., 2009).

The sequential spinup of the coupled climate model is detailed in Thornton et al. (2009), resulting in a global model with a stable climate and carbon cycle. In brief, a 1000-year preindustrial control simulation is followed by a transient simulation for the 1870–2099 period. We use 1870–1999 historical data to prescribe fossil fuel CO_2 emissions, and CO_2 emissions from the SRES A2 scenario for the period 2000–2099.

Phytoplankton response to climate change

I. Marinov et al.

The balance between fossil fuel emissions and net land and ocean CO_2 sources/sinks governs model atmospheric CO_2. The time-evolving simulated atmospheric CO_2 concentration is used in the atmospheric radiative transfer routines, and the land and ocean carbon sources/sinks respond to changes in simulated atmospheric CO_2, temperature and climate.

In our model, the diatom, small phytoplankton, and diazotroph chlorophyll and biomass (carbon) tracers each are determined by an equation of the form:

$$\frac{\partial P_x}{\partial t} + \nabla \cdot (\mathbf{u}P_x) - \nabla \cdot (K \cdot \nabla P_x) = \mu_x \cdot P - G(P_x) - m_x \cdot P_x - A(P_x) \tag{1}$$

where the left-hand side terms include advection and diffusion, and the biological terms on the right-hand side represent a source term due to growth and multiple sinks due to grazing (Holling type III), linear mortality and aggregation (square dependence on P_x).

The photosynthetic specific growth rate μ_x for each phytoplankton type x (diatoms, small phytoplankton and diazotrophs) is parameterized along the lines of Geider et al. (1998) as the product of a maximum phytoplankton C-specific growth rate μ_{ref} (referenced to 30°C), a temperature function (T_f), a nutrient limitation term (V_x) and a light availability function (L_x):

$$\mu_x = \mu_{ref} \cdot T_f \cdot V_x \cdot L_x \tag{2}$$

where μ_{ref} is $3\,d^{-1}$ for diatoms and small phytoplankton and $0.4\,d^{-1}$ for diazotrophs. The temperature function is the so-called Q10 function:

$$T_f = 2^{\left(\frac{T-30°C}{10°C}\right)} \tag{3}$$

While the temperature function is identical for all phytoplankton classes, different phytoplankton have different nutrient and light requirements (i.e., different V_x and L_x). For each of the three phytoplankton types, the most limiting nutrient governs the nutrient

limitation term as follows:

$$V_{\text{diat}} = \min\left(V_{\text{diat}}^{\text{Fe}}, V_{\text{diat}}^{\text{N}}, V_{\text{diat}}^{\text{SiO}_3}, V_{\text{diat}}^{\text{PO}_4}\right); \quad V_{\text{sp}} = \min\left(V_{\text{sp}}^{\text{Fe}}, V_{\text{sp}}^{\text{N}}, V_{\text{sp}}^{\text{PO}_4}\right);$$
$$V_{\text{diaz}} = \min\left(V_{\text{diaz}}^{\text{Fe}}, V_{\text{diaz}}^{\text{PO}_4}\right) \tag{4}$$

where $V_x^{\text{NO}_3} = \dfrac{\frac{\text{NO}_3}{K_x^{\text{NO}_3}}}{1 + \frac{\text{NO}_3}{K_x^{\text{NO}_3}} + \frac{\text{NH}_4}{K_x^{\text{NH}_4}}}; \quad V_x^{\text{NH}_4} = \dfrac{\frac{\text{NH}_4}{K_x^{\text{NH}_4}}}{1 + \frac{\text{NO}_3}{K_x^{\text{NO}_3}} + \frac{\text{NH}_4}{K_x^{\text{NH}_4}}}; \quad V_x^{\text{N}} = V_x^{\text{NO}_3} + V_x^{\text{NH}_4}$

$$\tag{5}$$

$$V_x^{\text{PO}_4} = \frac{\text{PO}_4}{\text{PO}_4 + K_x^{\text{PO}_4}}; \quad V_x^{\text{Fe}} = \frac{\text{Fe}}{\text{Fe} + K_x^{\text{Fe}}}; \quad V_x^{\text{SiO}_3} = \frac{\text{SiO}_3}{\text{SiO}_3 + K_x^{\text{SiO}_3}}$$

The light function L_x follows a modified form of the Geider et al. (1998) dynamic growth
model and includes photo-adaptation parameterized with adaptive Chl/C ratios:

$$L_x(I_{\text{par}}, T_f, V_x) = 1 - \exp\left(\frac{-\alpha_x \cdot \theta_x^c \cdot I_{\text{par}}}{\mu_{\text{ref}} V_x T_f}\right) \tag{6}$$

where α_x is the initial slope of the photosynthesis-irradiance (P-I) curve for phytoplank-
ton type x assumed to be 0.3 for diatoms and small phytoplankton, 0.036 for dia-
zotrophs and we defined

$$\theta_x^c = \left(\frac{\text{Chl}}{\text{C}}\right)_x \tag{7}$$

The ratio inside the exponential in Eq. (6) is a ratio between the instantaneous light
harvesting capacity $\alpha_x \theta_x^c I_{\text{par}}$ and the maximum photosynthetic rate $\mu_{\text{ref}} T_f V_x$. At high
light intensity, L_x approaches 1 and the photosynthetic growth rate (Eq. 2) approaches
its high limit $\mu_{\text{ref}} T_f V_x$. In low light, L_x approaches $\alpha_x \theta_x^c I_{\text{par}}/(\mu_{\text{ref}} T_f V_x)$ and the photosyn-
thetic rate approaches the linear relationship $\alpha_x \theta_x^c I_{\text{par}}$, which is independent of temper-
ature and nutrient limitation.

The largest loss term in Eq. (1) is due to grazing. The model has one zooplankton class with biomass Z that grazes adaptively on phytoplankton and large detritus; grazing follows a Holling type III functional response:

$$G(P_x) = u_x^{max} \cdot T_f \cdot \left(\frac{P_x^2}{P_x^2 + g_x^2} \right) Z \qquad (8)$$

5   Grazing is higher for small phytoplankton (larger maximum grazing rate u^{max}, see Table 1) and has the same temperature dependence via T_f as phytoplankton growth. Note that g_x is the same for small phytoplankton and diazotrophs, but smaller for diatoms (Table 1). Finally, the loss of biomass via aggregation of organic matter is parameterized as:

10    $\text{Aggreg}(P_x) = \min \left(a_x^{max} P_x, p_x P_x^2 \right) \qquad (9)$

3   Analysis and results

3.1   Ecological response to climate change

The three phytoplankton types compete for nutrients and light; the relative magnitude of the half-saturation K_x coefficients for the different species (Table 1) as well as the

15   nutrient saturated growth rate are essential for determining the outcome of competition. Because of their high affinity for nutrients and low resource requirements (lower K than diatoms, see Table 1), small phytoplankton dominate over diatoms and diazotrophs roughly from about 45° S to 45° N (Figs. 1 and 2). In the competition theory literature, organisms such as small phytoplankton that invest energy in adaptation to low nutri-

20   ent concentrations are called "K strategists". Diatom relative (or fractional) abundance is defined as the diatom biomass divided by the total phytoplankton biomass (Fig. 2). Diatoms, so-called "r strategists" in the ecological literature, are better at taking up

nutrients in low light, high nutrient environments and thus dominate in the highly seasonal high latitudes, where they exhibit higher nutrient saturated growth rates. Diatoms follow the vertical velocity patterns, with higher values in upwelling and convective regions such as the Equatorial Pacific, Southern Ocean and upwelling regions on the west coast of continents (Figs. 1a and 2). Light and temperature limited diazotrophs grow only in low latitude warm waters where they are limited by either iron or phosphorus and fix all the nitrogen they need from N_2 gas (Fig. 1e, f). Increased stratification results in a decrease in low latitude phosphate from 1980 to 2100 and a switch from iron to phosphorus limitation for Atlantic and Indian low latitude diazotrophs (figure not shown). Since diazotrophs have much smaller biomass concentrations than either the small phytoplankton or the diatoms, our analysis will mostly focus on the competition between the latter two species.

The nutrient limitation patterns for diatoms and small phytoplankton are similar (Fig. 1b, d), with nitrogen as the main limiting nutrient in the mid-latitude Atlantic and Indian Oceans for both diatoms and small phytoplankton, and iron the main limiting nutrient in the Pacific and in all ocean basins south of 45° S. Significant differences are found in the Arctic Ocean, where diatoms are nitrogen limited while small phytoplankton are iron limited, and in the Western Pacific Ocean, where diatoms are limited by silicon rather than iron, an essential nutrient necessary for diatom shell formation. Overall, the large-scale diatom and small phytoplankton nutrient limitation patterns change little with climate change over a century.

Model projections of climate driven changes in physics and nutrients are shown in Figs. 3 and 4. Figure 5 shows how climate driven changes in specific growth rate, biomass and carbon relative abundance (defined as the ratio of diatom to total phytoplankton biomass) differ for small phytoplankton and diatoms. Changes are approximated from the linear trends of the deseasonalized monthly data for 1980–2099 (multiplied by 120 years). Modest changes in grazing, linear mortality and aggregation ensure that climate induced changes in diatom carbon and relative abundance are driven primarily by changes in specific growth rates throughout most of the ocean (Fig. 5). We

proceed with a qualitative and a quantitative discussion of how large scale changes in nutrients, temperature and light influence differentially the specific growth rate and therefore the biomass of the different phytoplankton classes.

Climate change results in a warmer surface ocean and an increase in the strength of the global hydrological cycle, acting to freshen the surface ocean particularly at the poles (Fig. 3). The combination of warmer and fresher surface waters reduces surface water density and acts to increase the vertical stratification of the upper water column. Oceanic vertical stratification, expressed in Fig. 3b as the density difference between surface and 200 m, increases at most locations in the ocean with climate warming, and results in reduced supply of subsurface nutrients to the surface throughout most of the ocean. Decreasing nitrate supply over large areas in the Indian and Atlantic ocean north of 45° S (Fig. 4b) translates in decreases in diatom growth rate, biomass and abundance (Fig. 5b, e, h). In the high latitudes of the Northern Hemisphere, diatoms show a stronger negative response to nutrient decline, such that their relative fractional abundance decreases significantly (by 6 to 15%) north of about 40° N (Figs. 3e and 5h). Overall, we note a close correlation between diatom nutrient functional response and diatom biomass and abundance, as previously reported (e.g. Bopp et al., 2005). The shape of the zonal mean change in diatom relative abundance (Fig. 3e) is similar to that reported by Bopp et al. (2005).

A reduction in mixed layer depth (due to enhanced stratification) combines with shrinking ice cover (Fig. 3c) to increase light availability for phytoplankton in high latitudes, as discussed in previous work (e.g., Doney 2006a). Small phytoplankton show a stronger positive response than diatoms to increases in high latitude light availability, such that small phytoplankton growth rate, biomass and relative abundance increase both S of 60° S and N of 60° N (Fig. 5a, d, g).

Can we analytically separate the individual impacts of changing light, nutrients and temperature on phytoplankton growth rates? A first order Taylor expansion to the

specific growth rate around some initial state yields from Eq. (2):

$$\Delta\mu_x = \left.\frac{\partial\mu}{\partial I_{par}}\right|_{V_x,T_f\text{constant}} \cdot \Delta I_{par} + \left.\frac{\partial\mu}{\partial V_x}\right|_{I_{par},T_f\text{constant}} \cdot \Delta V_x + \left.\frac{\partial\mu}{\partial T_f}\right|_{I_{par},V_x\text{constant}} \cdot \Delta T_f \qquad (10)$$

Taking into account the fact that the light limitation function L_x is a function of I_{par}, V_x and T_f, we expand the terms in Eq. (10) as detailed in Appendix A and get:

$$\Delta\mu_x = \Delta\mu_x^{light} + \Delta\mu_x^{nutr} + \Delta\mu_x^{temp} \qquad (11)$$

The light function, nutrient and temperature contributions to the growth rate change are:

$$\Delta\mu_x^{light} = \alpha_x\theta_x^c I_{par} \cdot \left(\frac{\Delta I_{par}}{I_{par}} - \frac{\Delta V_x}{V_x} - \frac{\Delta T_f}{T_f}\right) \cdot \exp\left(\frac{-\alpha_x \cdot \theta_x^c \cdot I_{par}}{\mu_{ref}V_x T_f}\right) \qquad (12a)$$

$$\Delta\mu_x^{nutr} = \mu_{ref} \cdot T_f L_x \cdot \Delta V_x \qquad (12b)$$

$$\Delta\mu_x^{temp} = \mu_{ref} \cdot L_x V_x \cdot \Delta T_f \qquad (12c)$$

where I_{par}, V_x and T_f represent the initial state, and the Δ notation refers to small perturbations around this state. The growth rate terms (Eq. 12a–c) show the contribution of changes in light, nutrients and temperature to biomass changes. These terms, calculated from the linear trends in monthly light, nutrients and temperature for years 1980–2099, are illustrated in Fig. 6 for both diatoms and small phytoplankton. The average impact of temperature, nutrients, light and grazing on total biomass, as well as the fractional changes in zooplankton abundances, nitrate, iron and surface irradiance are illustrated over five different domains of the ocean in Fig. 7 (the 45° S–45° N biome) and Fig. 8 (the marginal sea-ice and the subpolar biomes). The marginal sea ice biomes are defined here as the Northern or Southern Hemisphere provinces covered by sea ice during some part of the year (but which are not permanently covered

by sea ice), averaged for years 1980–1999. The subpolar biomes are chosen here to correspond to all areas poleward of 45° N or 45° S not included in the marginal sea ice biome.

We make three immediate observations:

5   1. Climate driven decreases in nutrients have a larger impact on small phytoplankton specific growth rate than on diatom specific growth rate in the 45° S–45° N biome. The opposite is the case in the four high latitude biomes.

2. Climate driven changes in light, whether positive or negative, have a stronger impact on small phytoplankton than on diatom specific growth rate.

10   3. Increasing temperature increases small phytoplankton specific growth rate more than it increases diatoms specific growth rate.

In Sects. 3.2–3.4 we provide a mathematical analysis that can help us understand each of these three effects and test our predictions against the modeled climate simulations. We conclude with a detailed discussion of modeled ecology in each of these
15   biomes.

3.2   The critical nutrient theory

Let us assume that we are in a region in which both small phytoplankton and diatoms are limited by the same nutrient. Figure 9a, c shows the nutrient functional response V_x for diatoms and small phytoplankton as a function of the limiting nutrient, with higher
20   half saturation coefficient K_x values for diatoms resulting in lower values: $V_{sp} > V_{diat}$. The shape of the nutrient functional response ensures that there is a critical nutrient value above which the slope of V_{diat} is steeper than the slope of V_{sp} (Fig. 9b, d) such that for a given change in limiting nutrient ΔN, the resulting change in nutrient functional response is larger for diatoms than for small phytoplankton: $|\Delta V_{diat}| > |\Delta V_{sp}|$. Conversely,
25   for nutrient concentrations below the critical nutrient level, an increase (decrease) in the limiting nutrient will result in a larger increase (decrease) in nutrient functional response

for small phytoplankton than for diatoms: $|\Delta V_{sp}| > |\Delta V_{diat}|$ and therefore $|\Delta \mu_{sp}^{nutr}| > |\Delta \mu_{diat}^{nutr}|$. That is, below the critical nutrient level, a nutrient change ΔN has a larger effect on the growth rate of the plankton group with the low K value (small phytoplankton are influenced more strongly in low nutrient environments). Figure 10 shows that our critical nutrient theory predictions are well matched by our model results.

Mathematically, we consider the phytoplankton nutrient functional response for a generic limiting nutrient $V_x = N/(N + K_x)$ and calculate:

$$\frac{\partial V_x}{\partial N} = \frac{\partial}{\partial N}\left(\frac{N}{N + K_x^N}\right) = \frac{K_x^N}{\left(N + K_x^N\right)^2} \tag{13}$$

The critical nutrient value is achieved when the nutrient functional response slopes are equal

$$\frac{\partial V_{sp}}{\partial N} = \frac{\partial V_{diat}}{\partial N} \quad \text{implies} \quad \frac{K_{diat}^N}{(N + K_{diat}^N)^2} = \frac{K_{sp}^N}{(N + K_{sp}^N)^2}$$
$$\text{or} \quad N_{critical} = \sqrt{K_{diat}^N K_{sp}^N} \tag{14}$$

Then, as illustrated in Fig. 9b, d for a small change in nutrient ΔN:

$$N \leq N_{critical} \quad \text{implies} \quad \frac{\partial V_{sp}}{\partial N} \geq \frac{\partial V_{diat}}{\partial N} \quad \text{and} \quad \left|\Delta V_{sp}\right| \geq |\Delta V_{diat}| \tag{15}$$

and conversely

$$N \geq N_{critical} \quad \text{implies} \quad \frac{\partial V_{sp}}{\partial N} \leq \frac{\partial V_{diat}}{\partial N} \quad \text{and} \quad \left|\Delta V_{sp}\right| \leq |\Delta V_{diat}| \tag{16}$$

Note that the critical nutrient concept makes sense only for K_{sp} different from K_{diat}. In our model, the critical nutrient value for nitrate and iron limited regions are given by:

$$NO_{3critical} = \sqrt{K_{diat}^{NO_3} K_{sp}^{NO_3}} = 1.18 \text{ mmol } NO_3/m^3$$
$$Fe_{critical} = \sqrt{K_{diat}^{Fe} K_{sp}^{Fe}} = 95 \text{ nmol } Fe/m^3 \tag{17}$$

In regions in which nutrients are below a critical threshold, we write from Eq. (12b) $|\Delta\mu_{sp}^{nutr}|\geq|\Delta\mu_{diat}^{nutr}|$. If the nutrient term $\Delta\mu_x^{nutr}$ is large enough to dominate the total growth rate change such that $\Delta\mu_x\cong\Delta\mu_x^{nutr}$, a given change in the limiting nutrient will affect more small phytoplankton than diatoms, i.e., $|\Delta\mu_{sp}|\geq|\Delta\mu_{diat}|$.

5   Depending on how the critical iron and nitrate values compare with actual surface nutrient values (Fig. 4), we broadly distinguish two regimes: one in which efficient biology and reduced vertical mixing of nutrients ensure that limiting nutrients are below critical nutrient levels (Eq. 15), roughly corresponding to the 45° S–45° N band, and one in which nutrients are above the critical value (Eq. 16), roughly corresponding to

10   the high latitudes poleward of 45° S. These two regimes correspond respectively to the left hand side and the right hand side of the critical nutrient value in Fig. 9a–d. The predictions of our theory based on the actual nutrient values and nutrient limitation patterns in our model are shown in Fig. 10a.

Regime 1: 45° S to 45° N

15   In the Atlantic and Indian oceans north of 45° S, nitrate is the limiting nutrient for both diatoms and small phytoplankton and efficient biology draws down nutrients below the critical level, i.e. $NO_3 < NO_{3critical}$. Over most of the Pacific and everywhere in the Southern Ocean south of 45° S, Fe is low and the limiting nutrient, and $Fe < Fe_{critical}$. Our theory then implies that for a given temporal change in the limiting nutrient, the absolute

20   change in nutrient functional response should be larger for small phytoplankton than for diatoms: $|\Delta V_{sp}| > |\Delta V_{diat}|$ and therefore $|\Delta\mu_{sp}^{nutr}| > |\Delta\mu_{diat}^{nutr}|$.

In order to check our theory, we calculate $\Delta\mu_{sp}^{nutr}$ and $\Delta\mu_{diat}^{nutr}$ from the temporal linear trends for the time period 1980–2100 from model monthly data. The low and mid-latitude Atlantic and Indian oceans are primarily characterized by increased stratifica-

25   tion and decreased supply of nitrate to the ocean surface in a future climate, resulting in decreased phytoplankton nitrate functional response and decreased μ_x^{nutr}. Analysis of model results confirms that in this region the climate induced decreases in V_{sp} and

Title Page

Abstract | Introduction

Conclusions | References

Tables | Figures

|◄ | ►|

◄ | ►

Back | Close

Full Screen / Esc

Printer-friendly Version

Interactive Discussion

μ_{sp}^{nutr} are larger than the corresponding decreases in V_{diat} and μ_{diat}^{nutr} (Fig. 6a–c). Indeed, the regions of μ_{sp}^{nutr} versus μ_{diat}^{nutr} dominance shown in Fig. 10b are almost identical with those predicted by the theory (Fig. 10a). The critical nutrient theory predicts correctly that climate change has a larger impact on small phytoplankton growth rates compared to diatom growth rate in the low and midlatitude oceans (Fig. 7).

Regime 2: south of 45° S and north of 45° N

Phytoplankton are iron limited in the Southern Ocean south of 45° S, while both iron and nitrate limited in the Arctic and North Atlantic north of 45° N. Let us consider regions in which small phytoplankton and diatoms are limited by the same nutrient. Inefficient biology and a seasonal supply of nutrients from below ensure that the concentrations of limiting nutrients in these regions are higher than critical nutrient values. For a given change in the limiting nutrient, the change in nutrient functional response V_x is therefore larger for diatoms compared to small phytoplankton, and therefore $|\Delta\mu_{diat}^{nutr}|>|\Delta\mu_{sp}^{nutr}|$ (Figs. 6a–c and 8a–d).

Furthermore, because we are on the right hand side of the critical nutrient value in Fig. 9, nutrient functional response is close to saturation and its slope is small (Fig. 9b, d), i.e., $|\Delta V_x|$ small. We therefore expect that equivalent changes in nutrients result in smaller changes in phytoplankton specific growth rate compared to those observed in the 45° S–45° N domain. Since $|\Delta V_x|$ is small, we expect that throughout much of this domain $|\Delta\mu_x^{nutr}|$ is smaller than $\Delta\mu_x^{temp}$ or $\Delta\mu_x^{light}$. As discussed below and illustrated in Fig. 11e, f, temperature dominates the system in the 45° S–60° S band, while light becomes critical and governs the small phytoplankton bloom in the Antarctic marginal sea-ice zone, i.e. $\Delta\mu_x \cong \Delta\mu_x^{light}$.

Phytoplankton response to climate change

I. Marinov et al.

3.3 The impact of temperature on phytoplankton growth

Now we turn to analyzing the contribution of temperature to the growth rate, $\Delta\mu_x^{\text{temp}}$, as defined in Eq. (12c), for various phytoplankton species. Since the temperature term T_f (Eq. 3) is the same for all phytoplankton in the model it does not lead directly to differential effects on phytoplankton growth via changes in T_f in Eq. (12c). Rather, differences in the initial nutrient functional response V_x and light limitation function L_x contribute to differences in $\Delta\mu_x^{\text{temp}}$ between species.

For any y positive the function $f(y)=(1-e^{-a/y})\cdot y$ is monotonic and increasing, such that $y_1>y_2$ implies $f(y_1)>f(y_2)$. We now set $y_1=V_{\text{sp}}$ and $y_2=V_{\text{diat}}$. Small phytoplankton have lower half saturation coefficients and larger nutrient functional response than diatoms everywhere in the ocean, i.e., $V_{\text{sp}}>V_{\text{diat}}$. Since differences in θ_x^c/V_x are dominated by differences in V_x and $\alpha_{\text{diat}}=\alpha_{\text{sp}}$ we have:

$$\left(1-e^{-\alpha_{\text{sp}}\theta_{\text{sp}}^c I_{\text{par}}/(\mu_{\text{ref}}V_{\text{sp}}T_f)}\right)\cdot V_{\text{sp}} > \left(1-e^{-\alpha_{\text{diat}}\theta_{\text{diat}}^c I_{\text{par}}/(\mu_{\text{ref}}V_{\text{diat}}T_f)}\right)\cdot V_{\text{diat}}.$$

We recognize the terms in the parantheses as the light function terms L_{sp} and L_{diat}, and we can now write:

$$\mu_{\text{ref}}\cdot L_{\text{sp}}V_{\text{sp}} > \mu_{\text{ref}}\cdot L_{\text{diat}}V_{\text{diat}} \tag{18}$$

Temperature increases everywhere at the ocean surface with climate change such that ΔT_f is positive. Therefore, we predict from Eqs. (12c) and (18) that:

$$\Delta\mu_{\text{sp}}^{\text{temp}} > \Delta\mu_{\text{diat}}^{\text{temp}} > 0 \tag{19}$$

Increasing temperature acts to increase phytoplankton growth rate and biomass. Figures 6d, e, f, 7 and 8 confirm our prediction (19): a given increase in temperature preferentially increases small phytoplankton compared to diatoms in all ocean regions.

We next try to predict the regions where growth rate changes are dominated by nutrients rather than temperature, i.e. $|\Delta\mu_x^{\text{nutr}}|>|\Delta\mu_x^{\text{temp}}|$. From $V_x=N/(N+K_x)$ and Eq. (3)

we derive, assuming small changes in T and N:

$$\Delta V_x = \frac{K_x^N \cdot \Delta N}{(N + K_x^N)^2} \quad \text{and} \quad \Delta T_f = \frac{\ln 2}{10(°C)} \cdot T_f \cdot \Delta T \qquad (20)$$

where N corresponds to some average value of the limiting nutrient (nitrate, iron, silica or phosphate), T is temperature and K_x is the half saturation coefficient corresponding to a specific nutrient N and phytoplankton type x. Plugging in these relationships in Eq. (12b–c) we can show that:

$$|\Delta N| > \frac{N \cdot (N + K_x^N)}{K_x^N} \cdot \frac{\ln 2}{10(°C)} \cdot |\Delta T| \Leftrightarrow \left| \Delta \mu_x^{nutr} \right| > \left| \Delta \mu_x^{temp} \right| \qquad (21)$$

We use the 1980–2100 linear trends in the limiting nutrient and temperature to calculate ΔN and ΔT and we predict from the above equation the regions where growth rate change due to nitrate or iron should dominate over the growth rate change due to temperature for each of our phytoplankton types. These theoretically predicted regions (green regions in Fig. 11a ,b) match remarkably well the results of climate change projections (green regions in Fig. 11c, d). The model projected regions are calculated by comparing the 1980–2100 changes in μ_{diat}^{nutr} and μ_{diat}^{temp} and the changes in μ_{sp}^{nutr} and μ_{sp}^{temp}, respectively.

Equation (21) intuitively makes sense. The nutrient term dominates over the temperature term in the Atlantic and Pacific midlatitudes where the nitrate decrease is significant and the background nitrate values are rather small due to efficient biology. The temperature term dominates over the nutrient term in regions where the temperature increase is large (e.g., the Pacific midlatitudes) or where the background nutrients are large due to inefficient biology (such as most of the Southern Ocean and the Equatorial Pacific). Finally, since K_{sp} is smaller than K_{diat}, Eq. (21) suggests correctly that regions where changes in specific growth rate are dominated by temperature (i.e., $|\Delta \mu_x^{temp}| > |\Delta \mu_x^{nutr}|$) should occupy a larger area of the ocean for small phytoplankton

compared to diatoms (Fig. 11c, d). The situation becomes slightly more complex in the high latitudes where light is a strong limiting factor for growth, and climate induced changes in $\Delta\mu_x^{\text{light}}$ become larger than either $\Delta\mu_x^{\text{temp}}$ or $\Delta\mu_x^{\text{nutr}}$ for both diatoms and small phytoplankton, as illustrated in Fig. 11e, f. This is the subject of the next section.

Finally, we note that our model is parameterized such that temperature affects the rates of growth and grazing in the same direction, i.e., increasing temperature increases both biomass and grazing rates via T_f (Eqs. 2 and 8). Increases in the temperature growth term is therefore partly compensated in all domains by the increase in grazing term (Fig. 8a–d), so a small net increase in biomass occurs with increasing temperature. Because of differential grazing coefficients in Eq. (8), grazing has a larger impact on small phytoplankton biomass than on diatom biomass, compensating some of the small phytoplankton-diatom biomass differences induced by temperature effect on growth.

3.4 The impact of light on phytoplankton growth

Next we turn to analyzing the contribution of light to changes in growth rate, $\Delta\mu_x^{\text{light}}$, as defined in Eq. (12a), for various phytoplankton species. At high light (in low latitudes or in the summer) the exponential approaches zero and $\Delta\mu_x^{\text{light}}$ becomes small. At low light the exponential approaches its high limit $\alpha_x\theta_x^c I_{\text{par}}/(\mu_{\text{ref}}T_f V_x)$, and the resulting $\Delta\mu_x^{\text{light}}$ depends on the initial light levels, nutrients and temperature. We note an interesting contrast with the low light limit in μ_x, $\alpha_x\theta_x^c I_{\text{par}}$, which does not depend on nutrients or temperature. Figure 6g–i confirms that the impact of changing light on growth rate is larger in the (low light) high latitudes compared to low latitudes.

The light contribution to the growth rate change $\Delta\mu_x^{\text{light}}$ dominates the nutrient or temperature contributions in the Arctic and Antarctic marginal sea-ice biomes (Fig. 8a and b and also Fig. 11e and f). According to Eq. (12a), the sign of the light limitation

contribution to the growth rate, $\Delta\mu_x^{\text{light}}$, is given by the sign of

$$S = \left(\frac{\Delta I_{\text{par}}}{I_{\text{par}}} - \frac{\Delta V_x}{V_x} - \frac{\Delta T_{\text{f}}}{T_{\text{f}}} \right)$$

and thus depends on the relative fractional increases of light, nutrient functional response and temperature function. An increase in irradiance I_{par} will naturally act to
increase phytoplankton growth rate, while increases in nutrient functional response and temperature will act to decrease the growth rate. A close analysis confirmed by Fig. 8 shows that light enhances the growth of small phytoplankton and diatoms in both the Arctic and the Antarctic ice regions (i.e., $\mu_{\text{sp}}^{\text{light}}$ and $\mu_{\text{diat}}^{\text{light}}$ positive) primarily because of an increase in I_{par} from 1980 to 2100 (partly due to dwindling ice cover),
combined with a pronounced decrease in limiting nutrients and thus ΔV_x in the Arctic. Additionally, $\Delta\mu_x^{\text{light}}$ decreases over most of the Pacific because of enhanced warming ($\Delta T_{\text{f}} > 0$), while it increases locally in the North Pacific and North Atlantic (around $30°–45°$ N), Equatorial Atlantic and North Indian Ocean largely due to decreased nutrient functional response ($\Delta V_x < 0$).

We next compare the terms $\Delta\mu_{\text{diat}}^{\text{light}}$ and $\Delta\mu_{\text{sp}}^{\text{light}}$. Smaller nitrate and iron half saturation coefficients for small phytoplankton and very similar nutrient limitation patterns (Fig. 1) ensure that $V_{\text{sp}} > V_{\text{diat}}$ everywhere. Since differences in θ_x^c/V_x are dominated by differences in V_x, we can write:

$$\exp\left(\frac{-\alpha_{\text{sp}} \cdot \theta_{\text{sp}}^c \cdot I_{\text{par}}}{\mu_{\text{ref}} V_{\text{sp}} T_{\text{f}}} \right) > \exp\left(\frac{-\alpha_{\text{diat}} \cdot \theta_{\text{diat}}^c \cdot I_{\text{par}}}{\mu_{\text{ref}} V_{\text{diat}} T_{\text{f}}} \right).$$

Assuming that differences in S_{diat} and S_{sp} are small relative to the above inequality, we predict that overall changes in the light limitation growth terms (Eq. 12a) are more pronounced for small phytoplankton than for diatoms:

$$\left| \Delta\mu_{\text{sp}}^{\text{light}} \right| > \left| \Delta\mu_{\text{diat}}^{\text{light}} \right| \tag{22}$$

Analysis of the light limitation growth terms in Fig. 6g–i and Figs. 7–8 confirms the validity of Eq. (22) over most of the ocean. A given change in light will therefore affect more small phytoplankton than diatoms. An implication of Eq. (22) is that in the Arctic and Antarctic marginal sea-ice biomes in which light I_{par} increases with climate change, $S > 0$ and $\Delta\mu_{sp}^{light} > \Delta\mu_{diat}^{light} > 0$. Here, $\Delta\mu_x^{light}$ is large enough to dominate the total growth rate change and small phytoplankton biomass preferentially increases over diatom carbon, as confirmed by Fig. 8a, b. Increasing cloud cover decreases surface irradiance in the subtropics. Light becomes more limiting for small phytoplankton, i.e. μ_{sp}^{light} decreases more than μ_{diat}^{light} (Fig. 6g–i). This enhances the observed trend in $\Delta\mu_x^{nutr}$ whereby nutrients become more limiting for small phytoplankton, further reducing small phytoplankton over diatoms (Fig. 7).

3.5 On the relative contribution of small phytoplankton and diatoms to the carbon pool

We have argued above that climate driven temperature, light, and low-mid latitude nutrient changes affect small phytoplankton biomass more than diatom biomass. It is, however, not straight-forward to extrapolate our arguments to relative abundances. Figures 7 and 8 illustrate the complex relationship between biomass and relative (or fractional) abundance. Assuming that diazotrophs are a negligible contribution to the total carbon pool, the time change in the fractional abundance of diatoms can be written, after a couple of basic manipulations, as:

$$\Delta\left(\frac{P_{diat}}{P_{sp} + P_{diat}}\right) = \ldots = \frac{P_{diat}P_{sp}}{\left(P_{sp} + P_{diat}\right)^2}\left(\frac{\Delta P_{diat}}{P_{diat}} - \frac{\Delta P_{sp}}{P_{sp}}\right) \tag{23}$$

The relative (or fractional) abundance of diatoms depends on the difference between the relative diatom biomass change ($\Delta P_{diat}/P_{diat}$) and the relative small phytoplankton change ($\Delta P_{sp}/P_{sp}$).

Phytoplankton response to climate change

I. Marinov et al.

Title Page

Abstract	Introduction
Conclusions	References
Tables	Figures

| ◄◄ | ►► |
| ◄ | ► |

| Back | Close |

Full Screen / Esc

Printer-friendly Version

Interactive Discussion

Over most of the 45° S–45° N region nutrient decrease (due to climate change) results in a larger absolute decrease in small plankton biomass compared to diatoms: $|\Delta P_{sp}| > |\Delta P_{diat}|$. However, over most of this region small phytoplankton dominate $P_{sp} \gg P_{diat}$, such that the relative biomass decrease is actually smaller for small phytoplankton: $|\Delta P_{sp}/P_{sp}| < |\Delta P_{diat}/P_{diat}|$ and from Eq. (23):

$$\text{Sign}\left[\Delta\left(\frac{P_{diat}}{P_{sp}+P_{diat}}\right)\right] = \text{Sign}\left[\frac{\Delta P_{diat}}{P_{diat}}\right] \tag{24}$$

We therefore expect on average, in the 45° S–45° N biome, a decrease in the proportion of diatoms and an increase in the proportion of small phytoplankton to total biomass with climate change in the low and mid-latitude regime (Figs. 3e and 7). If interspecies competition is defined with respect to relative change, then we note a decrease in the competitiveness of diatoms (relative to small phytoplankton) with climate change in the low to mid latitudes, in agreement with previous modeling studies (Bopp et al., 2005), laboratory and field data (Jin et al., 2006; Cermeno et al., 2009). We also note conceptual agreement with Agawin et al. (2000) and Moran et al. (2010), who noticed a shift in the total community to smaller sizes with an increase in temperature.

In the light limited marginal sea-ice biomes, an increase in light acts to primarily increase P_{sp}, $\Delta P_{sp} > \Delta P_{diat}$. Since P_{diat} is of the same order of magnitude or larger than P_{sp}, $\Delta P_{sp}/P_{sp} > \Delta P_{diat}/P_{diat}$ and therefore from Eq. (23):

$$\text{Sign}\left[\Delta\left(\frac{P_{diat}}{P_{sp}+P_{diat}}\right)\right] = \text{Sign}\left[-\frac{\Delta P_{sp}}{P_{sp}}\right] \tag{25}$$

In conclusion, increases in light and temperature in the marginal sea-ice biomes act to decrease the proportion of diatoms and increase the proportion of small phytoplankton to total biomass (Fig. 8a, b).

4 Discussion

Our mathematical analysis is a useful tool for diagnosing and predicting the behavior of ocean ecology with future climate change in models governed by the Geider et al. (1998) type formalism for plant photosynthesis. The exact forms of our derived Eq. (12a–c) and the theoretical analysis can easily be tailored to take into account modifications of this formalism. Our critical nutrient theory should hold as long as Michaelis-Menten type nutrient functional response is assumed. Assuming a multiplicative growth equation (Eq. 2), we demonstrated that climate driven increases in temperature and changes in light always preferentially affect small phytoplankton compared to diatoms. The increase in temperature and light are most important in the Subpolar Southern Ocean biome and the marginal sea-ice biomes, respectively, where they lead to increases in small phytoplankton biomass and relative abundance. Below we analyze separately the marginal sea-ice biomes and the subpolar biomes.

In the marginal sea-ice biome, light limitation is important, with diatoms and small phytoplankton blooming in the spring and summer when light allows it. Decreasing ice cover and increased stratification with global warming result in more light availability in spring and summer, and are primarily responsible for the observed ecosystem changes. In the North Atlantic- Arctic Ice biome, small phytoplankton are iron limited in fall and winter and nitrogen limited in spring and summer, while diatoms are nitrogen limited at all times. More stratification makes nitrate more limiting to both species in spring and summer. Temperature dependent increases in grazing rates compensates largely for temperature dependent increases in phytoplankton growth (increased linear loss and aggregation play a smaller role; Fig. 8a). At the elevated nutrient background levels, small phytoplankton are less sensitive to the decrease in nitrogen than diatoms, as expected from the critical nutrient theory. Small phytoplankton also react better to the increase in light availability, in agreement with Eq. (22). As a consequence, small phytoplankton increase with climate change, while diatom spring and summer blooms decrease primarily due to nutrient decline.

In the marginal sea-ice biome adjacent to Antarctica both small phytoplankton and diatoms are iron and light limited. The observed increase of small phytoplankton is dominated by increases in light availability primarily due to retreating sea ice (Fig. 8b).

Increased diatom grazing, loss and aggregation compensate for the increase in light and contribute to an average decrease in diatom biomass and relative abundance. Small phytoplankton increase dominates such that total phytoplankton biomass and total zooplankton biomass both increase in time. In summary, a stronger response to increased light makes small phytoplankton more competitive in the ice biomes relative to diatoms.

In the Subpolar North Atlantic, diatoms are primarily nitrate (and in some locations iron) limited, while small phytoplankton are primarily light limited. Stronger stratification implies a thinner mixed layer depth and a decrease in surface nitrate by $1–2\,\mathrm{mmol/m^3}$. In this high nutrient regime nitrate decrease preferentially limits diatoms (in agreement with our theory, Sect. 3.2), such that diatom biomass and relative abundance both decrease (Fig. 8c). Minimal changes in small phytoplankton are due to compensating effects on biomass growth of increased temperature on one hand and increased grazing, decreased nutrients and light on the other. Small zooplankton decrease follows the diatom decrease.

In the Southern Ocean subpolar biome the increase in diatom growth rate and biomass is clearly dominated by the increasing temperature term (Fig. 8d). Both surface and average mixed layer light decrease in this region. The decrease is most pronounced at the surface (a 47% reduction), suggesting increased cloudiness. In agreement with our theoretical analysis (Eq. 22) decreasing light preferentially limits small phytoplankton, ultimately driving, together with increased grazing on small phytoplankton, a decrease in small phytoplankton biomass. Zooplankton increase slightly in the Subpolar South Atlantic due to the diatom increase and decrease slightly in the Subpolar South Pacific due to the small phytoplankton decrease. In the biome average there is almost no change in zooplankton. More sensitivity to temperature increase and less sensitivity to a decrease in light make diatoms more competitive than small

phytoplankton.

We conclude that climate driven changes in nutrients, temperature and light have regionally varying and sometimes counterbalancing impacts on phytoplankton biomass and structure, with nutrients and temperature dominating in the 45° S–45° N band and light-temperature effects dominating in the marginal sea-ice and subpolar regions. If phytoplankton nutrient functional response in the ocean follows Michaelis-Menten kinetics, we predict that there should be a critical nutrient threshold, below (above) which any nutrient changes will affect more (less) small phytoplankton biomass than diatom biomass. This nutrient threshold broadly corresponds to 45° S and 45° N, poleward of which biology is inefficient, vertical mixing and therefore nutrients are high and equatorward of which biology is inefficient, vertical mixing is reduced and therefore nutrients are low. The critical nutrient theory is a most useful predictor of carbon changes in the 45° S–45° N band, where intensified climate drives nutrient depletion, which decreases small phytoplankton biomass more strongly than diatom biomass (Fig. 7). In high latitudes, the impact of nutrient decrease on phytoplankton biomass (as expressed through the nutrient contribution to the change in growth rate) is more significant for diatoms than for small phytoplankton, and contributes to diatom decay in the northern marginal sea-ice and subpolar biomes.

Unfortunately, the large-scale distribution of phytoplankton and its temporal variability is not yet well constrained by observations. Mapping major phytoplankton distributions from satellite (e.g. Alvain et al., 2008) and in-situ measurements is essential for a better understanding of the present and future ocean ecology and carbon cycle. Such studies will provide constraints on theoretical developments such as ours and will help us improve the representation of ocean biology in climate models. In turn, a deeper theoretical understanding of the basic ecological equations used in global models can help us predict future ecological and biogeochemical climate-driven shifts and point to critical processes that need targeted observations. It would be interesting to explore the existence of the "critical nutrient" biogeochemical boundary in the real ocean.

Phytoplankton response to climate change

I. Marinov et al.

Title Page

Abstract	Introduction
Conclusions	References
Tables	Figures

|◄ | ►|

◄ | ►

Back | Close

Full Screen / Esc

Printer-friendly Version

Interactive Discussion

Appendix A

We are interested in how the growth rate of a given phytoplankton species $\mu_x = \mu_{\text{ref}} \cdot T_f \cdot V_x \cdot L_x$ changes with climate change. A first order Taylor approximation to the specific growth rate yields:

$$\Delta \mu_x = \left. \frac{\partial \mu}{\partial I_{\text{par}}} \right|_{V_x, T_f ct} \cdot \Delta I_{\text{par}} + \left. \frac{\partial \mu}{\partial V_x} \right|_{I_{\text{par}}, T_f ct} \cdot \Delta V_x + \left. \frac{\partial \mu}{\partial T_f} \right|_{I_{\text{par}}, V_x ct} \cdot \Delta T_f \tag{A1}$$

Taking into account the fact that the light limitation function L_x is a function of I_{par}, V_x and T_f, and using the shorthand $d_x = (\alpha_x \cdot \theta_x^c)/\mu_{\text{ref}}$ the expansion of each of the above three terms gives:

$$\Delta \mu_x / \mu_{\text{ref}} = d_x \cdot \exp\left(\frac{-d_x \cdot I_{\text{par}}}{V_x T_f}\right) \cdot \Delta I_{\text{par}} + \left[T_f L_x - V_x T_f \cdot \frac{d_x \cdot I_{\text{par}}}{T_f V_x^2} \exp\left(\frac{-d_x \cdot I_{\text{par}}}{V_x \cdot T_f}\right) \right] \cdot \Delta V_x$$
$$+ \left[L_x V_x - V_x T_f \cdot \frac{d_x \cdot I_{\text{par}}}{V_x \cdot T_f^2} \exp\left(\frac{-d_x \cdot I_{\text{par}}}{V_x \cdot T_f}\right) \right] \cdot \Delta T_f \tag{A2}$$

where now I_{par}, V_x and T_f are some mean value and deltas are small deviations from this mean. Since we are considering only the first order Taylor approximation, quadratic and higher terms in delta were dropped. We rearrange the above equation as follows:

$$\Delta \mu_x / \mu_{\text{ref}} = \left[d_x \cdot \exp\left(\frac{-d_x \cdot I_{\text{par}}}{V_x T_f}\right) \cdot \Delta I_{\text{par}} - V_x T_f \cdot \frac{d_x \cdot I_{\text{par}}}{T_f V_x^2} \exp\left(\frac{-d_x \cdot I_{\text{par}}}{V_x T_f}\right) \cdot \Delta V_x \right.$$
$$\left. - V_x T_f \cdot \frac{d_x \cdot I_{\text{par}}}{V_x \cdot T_f^2} \exp\left(\frac{-d_x \cdot I_{\text{par}}}{V_x T_f}\right) \cdot \Delta T_f \right] + T_f L_x \cdot \Delta V_x + L_x V_x \cdot \Delta T_f \tag{A3}$$

or after further manipulation:

$$\Delta \mu_x / \mu_{\text{ref}} = \left[d_x \cdot I_{\text{par}} \cdot \left(\frac{\Delta I_{\text{par}}}{I_{\text{par}}} - \frac{\Delta V_x}{V_x} - \frac{\Delta T_f}{T_f} \right) \cdot \exp\left(\frac{-d_x \cdot I_{\text{par}}}{V_x T_f}\right) \right]$$
$$+ T_f L_x \cdot \Delta V_x + L_x V_x \cdot \Delta T_f \tag{A4}$$

The three terms on the right hand side represent the light function, nutrient and temperature contributions to the growth rate change, respectively, i.e.

$$\Delta\mu_x = \Delta\mu_x^{\text{light}} + \Delta\mu_x^{\text{nutr}} + \Delta\mu_x^{\text{temp}} \tag{A5}$$

References

Agawin, N. S. R., Duarte, C. M., and Agustí, S.: Nutrient and temperature control of the contribution of picoplankton to phytoplankton biomass and production, Limnol. Oceanogr., 45, 591–600, 2000.

Alvain, S., Moulin, C., Dandonneau, Y., et al.: Seasonal distribution and succession of dominant phytoplankton groups in the global ocean: a satellite view, Global Biogeochem. Cy., 22(3), GB3001, doi:10.1029/2007GB003154, 2008.

Armstrong, R. A., Lee, C., Hedges, J. I., Honjo, S., and Wakeham, S. G.: A new, mechanistic model for organic carbon fluxes in the ocean based on the quantitative association of POC with ballast minerals, Deep-Sea Res. Pt. II, 49, 219–236, 2002.

Aumont, O., Maier-Reimer, E., Blain, S., et al.: An ecosystem model of the global ocean including Fe, Si, P colimitations, Global Biogeochem. Cy., 17(2), GB1060, doi:10.1029/2001GB001745, 2003.

Bopp, L., Aumont, O., Cadule, P., et al.: Response of diatoms distribution to global warming and potential implications: a global modeling study, Geophys. Res. Lett., 32(19), L19606, doi:10.1029/2005GL023653, 2005.

Bopp, L., Monfray, P., Aumont, O., et al.: Potential impact of climate change on marine export production, Global Biogeochem. Cy., 15, 81–99, 2001.

Boyd, P. W. and Doney, S. C.: Modelling regional responses by marine pelagic ecosystems to global climate change, Geophys. Res. Lett. 29(16), 1806, doi:10.1029/2001GL014130, 2002.

Cermeno, P., Dutkiewicz, S., Harris, R. P., et al.: The role of nutricline depth in regulating the ocean carbon cycle, P. Natl. Acad. Sci. USA, 105, 20344, doi:10.1073/pnas.0811302106, 2008.

Collins, W. D., Bitz, C. M., Blackmon, M. L., et al.: The Community Climate System Model Version 3 (CCSM3), J. Climate, 19(11), 2122–2143, 2006a.

Collins, W. D., Rasch, P. J., Boville, B. A., et al.: The Formulation and Atmospheric simulation of the Community Atmosphere Model Version 3 (CAM3), J. Climate, 19(11), 2144–2161, 2006b.

Doney, S. C., Lima, I., Moore, J. K., Lindsay, K., Behrenfeld, M. J., Westberry, T. K., Mahowald, N., Glover, D. M., and Takahashi, T.: Skill metrics for confronting global upper ocean ecosystem-biogeochemistry models against field and remote sensing data, J. Marine Syst., 76, 95–112, doi:10.1016/j.jmarsys.2008.05.015, 2009.

Doney, S. C.: Plankton in a warmer world, Nature, 444, 695–696, 2006a.

Doney, S. C., Lindsay, K., Fung, I., et al.: Natural variability in a stable, 1000-yr global coupled climate-carbon cycle simulation, J. Climate, 19(13), 3033–3054, 2006b.

Falkowski, P. G., Barber, R. T., and Smetacek, V.: Biogeochemical controls and feedbacks on ocean primary production, Science, 281(5374), 200–206, 1998.

Falkowski, P. G., Katz, M. E., Knoll, A. H., et al.: The evolution of modern eukaryotic phytoplankton, Science, 305, 354–360, 2004.

Field, C. B., Behrenfeld, M. J., Randerson, J. T., and Falkowski, P.: Primary production of the biosphere: Integrating terrestrial and oceanic components, Science, 281(537), 237–240, 1998.

Follows, M. J., Dutkiewicz, S., Grant, S., and Chisholm, S. W.: Emergent biogeography of microbial communities in a model ocean, Science, 315, 1843–1846, 2007.

Geider, R. J., MacIntyre, H. L., and Kana, T. M.: A dynamic regulatory model of phytoplankton acclimation to light, nutrients, and temperature, Limnol. Oceanogr., 43, 679–694, 1998.

Gent, P. R. and McWilliams, J. C.: Isopycnal mixing in ocean circulation models, J. Phys. Oceanogr., 20(1), 150–155, 1990.

Jin, X., Gruber, N., Dunne, J. P., Sarmiento, J. L., and Armstrong, R. A.: Diagnosing the contribution of phytoplankton functional groups to the production and export of particulate organic carbon, $CaCO_3$, and opal from global nutrient and alkalinity distributions, Global Biogeochem. Cy., 20, GB2015, doi:10.1029/2005GB002532, 2006.

Large, W. G., McWilliams, J. C., and Doney, S. C.: Oceanic vertical mixing: a review and

a model with a nonlocal boundary layer parameterization, Rev. Geophys., 32(4), 363–403, 1994.

Le Quere, C., Aumont, O., Monfray, P., et al.: Propagation of climatic events on ocean stratification, marine biology, and CO_2: case studies over the 1979–1999 period, J. Geoph. Res., 108, C12, 3375, doi:10:1029/2001JC000920, 2003.

Le Quere, C., Harrison, S. P., Prentice, I. C., et al.: Ecosystem dynamics based on plankton functional types for global ocean biogeochemistry models, Glob. Change Biol., 11, 2016–2040, 2005.

Lima, I. D. and Doney, S. C.: A three-dimensional, multinutrient, and size-structured ecosystem model for the North Atlantic, Global Biogeochem. Cy., 18(3), GB3019, doi:1029/2003GB002146, 2004.

Moore, J. K. and Braucher, O.: Sedimentary and mineral dust sources of dissolved iron to the world ocean, Biogeosciences, 5, 631–656, doi:10.5194/bg-5-631-2008, 2008.

Moore, J. K., Doney, S. C., Lindsay, K., et al.: Nitrogen fixation amplifies the ocean biogeochemical response to decadal timescale variations in mineral dust deposition, Tellus B, 58(5), 560–572, 2006.

Moore, J. K., Doney, S. C., and Lindsay, K.: Upper ocean ecosystem dynamics and iron cycling in a global three-dimensional model, Global Biogeochem. Cy., 18, GB4028, doi:10.1029/2004GB002220, 2004.

Moore, J. K., Doney, S. C., Kleypas, J. C., Glover, D. M., and Fung, I. Y.: An intermediate complexity marine ecosystem model for the global domain, Deep-Sea Res. Pt. II, 49, 403–462, 2002.

Moran, X. A. G., Lopez-Urrutia, A., Calvo-Diaz, A., et al.: Increasing importance of small phytoplankton in a warmer ocean, Glob. Change Biol., 16(3), 1137–1144, 2010.

Najjar, R. G., Jin, X., Louanchi, F., et al.: Impact of circulation on export production, dissolved organic matter and dissolved oxygen in the ocean: results from OCMIP-2, Global Biogeochem. Cy., 21(3), GB3007, doi:10.1029/2006GB002857, 2007.

Sarmiento, J. L., Slater, R., Barber, R., et al.: Response of ocean ecosystems to climate warming, Global Biogeochem. Cy., 18(3), GB3003, doi:10.1029/2003GB002134, 2004.

Schmittner, A., Oschlies, A., Giraud, X., et al.: A global model of the marine ecosystem for long-term simulations: Sensitivity to ocean mixing, buoyancy forcing, particle sinking, and dissolved organic matter cycling, Global Biogeochem. Cy., 19, GB3004, doi:10.029/2004GB002283, 2005.

Phytoplankton response to climate change

I. Marinov et al.

Title Page

Abstract	Introduction
Conclusions	References
Tables	Figures

◄ | ►

◄ | ►

Back | Close

Full Screen / Esc

Printer-friendly Version

Interactive Discussion

Smetacek V.: Diatoms and the ocean carbon cycle, Protist, 150, 25–32, 1999.

Smith, R. D. and Gent, P. R.: Reference manual for the Parallel ocean Program (POP), ocean component of the Community Climate System Model (CCSM2.0 and 3.0). Tech. Rep. LA-UR-02-2484, Los Alamos National Laboratory, available at: http://www.ccsm.ucar.edu/models/ccsm3.0/pop, 2002.

Steinacher, M., Joos, F., Frölicher, T. L., Bopp, L., Cadule, P., Cocco, V., Doney, S. C., Gehlen, M., Lindsay, K., Moore, J. K., Schneider, B., and Segschneider, J.: Projected 21st century decrease in marine productivity: a multi-model analysis, Biogeosciences, 7, 979–1005, doi:10.5194/bg-7-979-2010, 2010.

Thornton, P. E., Doney, S. C., Lindsay, K., Moore, J. K., Mahowald, N., Randerson, J. T., Fung, I., Lamarque, J.-F., Feddema, J. J., and Lee, Y.-H.: Carbon-nitrogen interactions regulate climate-carbon cycle feedbacks: results from an atmosphere-ocean general circulation model, Biogeosciences, 6, 2099–2120, doi:10.5194/bg-6-2099-2009, 2009.

Yeager, S. G., Shields, C. A., Large, W. G., and Hack, J. J.: The low-resolution CCSM3, J. Climate, 19, 2545–2566, 2006.

Phytoplankton response to climate change

I. Marinov et al.

Title Page

Abstract | Introduction

Conclusions | References

Tables | Figures

|◄ | ►|

◄ | ►

Back | Close

Full Screen / Esc

Printer-friendly Version

Interactive Discussion

Table 1. Model parameters.

Parameter	Value	Units	Definition
α	0.3	$\mathrm{mmol\,C\,m^2\,(mg\,Chl\,W\,d)^{-1}}$	Initial slope of P-I curve
$\mu_{\mathrm{ref}}^{\mathrm{sp}}, \mu_{\mathrm{ref}}^{\mathrm{diat}}$	3	$\mathrm{d^{-1}}$	Max. small phytoplankton and diatom specific growth rates at T_{ref}
$\mu_{\mathrm{ref}}^{\mathrm{diaz}}$	0.4	$\mathrm{d^{-1}}$	Max. diazotrophs C specific growth rate at T_{ref}
$K_{\mathrm{sp}}^{\mathrm{NO_3}}$	0.5	$\mathrm{mmol\,N\,m^{-3}}$	Small phyto. NO_3 half saturation coefficient
$K_{\mathrm{sp}}^{\mathrm{NH_4}}$	0.005	$\mathrm{mmol\,N\,m^{-3}}$	Small phyto. NH_4 half saturation coefficient
$K_{\mathrm{sp}}^{\mathrm{Fe}}$	6×10^{-5}	$\mathrm{mmol\,Fe\,m^{-3}}$	Small phyto. Fe half saturation coefficient
$K_{\mathrm{sp}}^{\mathrm{PO_4}}$	3.125×10^{-4}	$\mathrm{mmol\,Fe\,m^{-3}}$	Small phyto. Fe half saturation coefficient
$K_{\mathrm{diat}}^{\mathrm{NO_3}}$	2.5	$\mathrm{mmol\,N\,m^{-3}}$	Diatom NO_3 half saturation coefficient
$K_{\mathrm{diat}}^{\mathrm{NH_4}}$	0.08	$\mathrm{mmol\,N\,m^{-3}}$	Diatom NH_4 half saturation coefficient
$K_{\mathrm{diat}}^{\mathrm{Fe}}$	1.5×10^{-4}	$\mathrm{mmol\,Fe\,m^{-3}}$	Diatom Fe half saturation coefficient
$K_{\mathrm{diat}}^{\mathrm{PO_4}}$	0.005	$\mathrm{mmol\,PO_4\,m^{-3}}$	Diatom PO_4 half saturation coefficient
$K_{\mathrm{diat}}^{\mathrm{SiO_3}}$	1	$\mathrm{mmol\,SiO_3\,m^{-3}}$	Diatom Si half saturation coefficient
$K_{\mathrm{diaz}}^{\mathrm{Fe}}$	1×10^{-4}	$\mathrm{mmol\,Fe\,m^{-3}}$	Diazotrophs Fe half saturation coefficient
$K_{\mathrm{diaz}}^{\mathrm{PO_4}}$	0.005	$\mathrm{mmol\,PO_4\,m^{-3}}$	Diazotrophs PO_4 half saturation coefficient
$u_{\mathrm{sp}}^{\mathrm{max}}$	2.75	$\mathrm{d^{-1}}$	Max zoo growth rate on small phytopl at $30\,^\circ$C
$u_{\mathrm{diat}}^{\mathrm{max}}$	2.07	$\mathrm{d^{-1}}$	Max zoo growth rate on diatoms at $30\,^\circ$C
$u_{\mathrm{diaz}}^{\mathrm{max}}$	1.2	$\mathrm{d^{-1}}$	Max zoo growth rate on diazotrophs at $30\,^\circ$C
m_{z}	0.1	$\mathrm{d^{-1}}$	Zooplankton linear mortality rate
$a_{\mathrm{sp}}^{\mathrm{max}}$	0.2	$\mathrm{d^{-1}}$	Max. aggregation rate for small phyto
$a_{\mathrm{diat}}^{\mathrm{max}}$	0.2	$\mathrm{d^{-1}}$	Max. aggregation rate for diatoms
$a_{\mathrm{diat}}^{\mathrm{min}}$	0.01	$\mathrm{d^{-1}}$	Min. aggregation rate for diatoms
$g_{\mathrm{sp}}, g_{\mathrm{diaz}}$	1.05	$\mathrm{mmol\,C\,m^{-3}}$	Zooplankton grazing on small phytoplankton and diazotrophs
g_{diat}	0.9×1.05	$\mathrm{mmol\,C\,m^{-3}}$	Zooplankton grazing on diatoms
$p_{\mathrm{sp}}, p_{\mathrm{diat}}$	0.009	$\mathrm{(mmol\,C)^{-1}\,m^3\,d^{-1}}$	Small phytoplankton/diatom quadratic mortality rate

Title Page

Abstract	Introduction
Conclusions	References
Tables	Figures

◄◄   ►►

◄   ►

Back   Close

Full Screen / Esc

Printer-friendly Version

Interactive Discussion

Discussion Paper | Discussion Paper | Discussion Paper | Discussion Paper
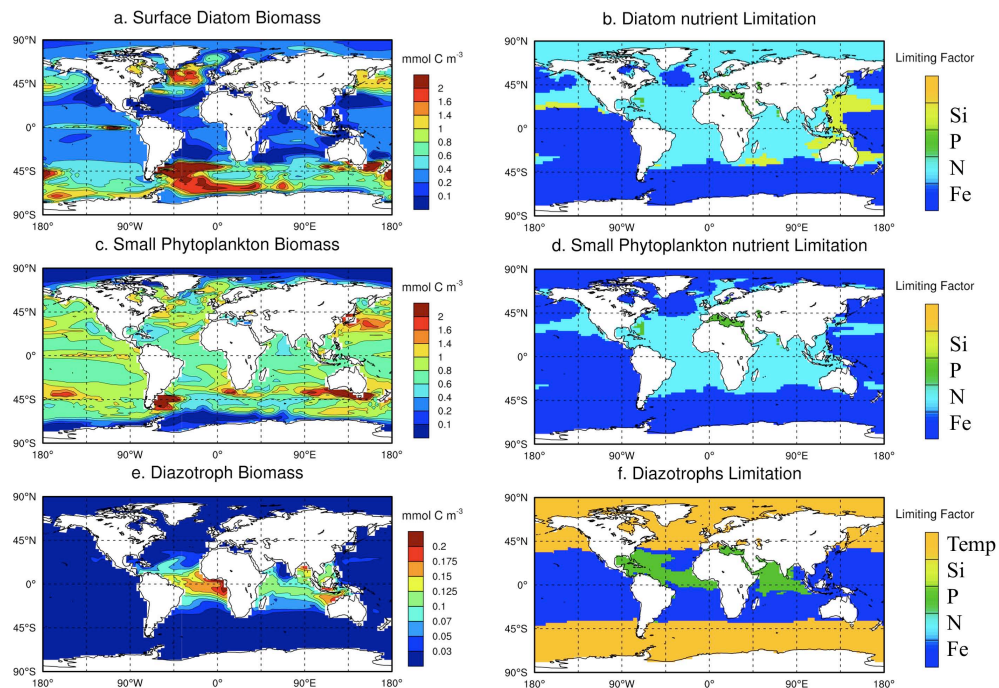
Fig. 1. Global maps of **(a, c, e)** diatom, small phytoplankton and diazotroph chlorophyll in mg Chl/m^3 as well as **(b, d, f)** the corresponding limiting nutrients averaged over the control period, years 1980–1999.
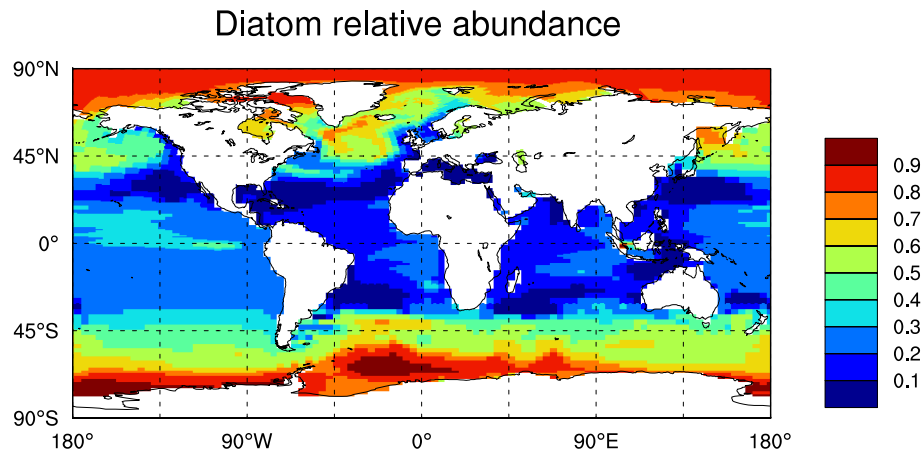
Diatom relative abundance

Fig. 2. Diatom relative abundance (no units) defined as the fractional contribution of diatom biomass to phytoplankton biomass, averaged for years 1980–1999.

Full Screen / Esc

Printer-friendly Version

Interactive Discussion
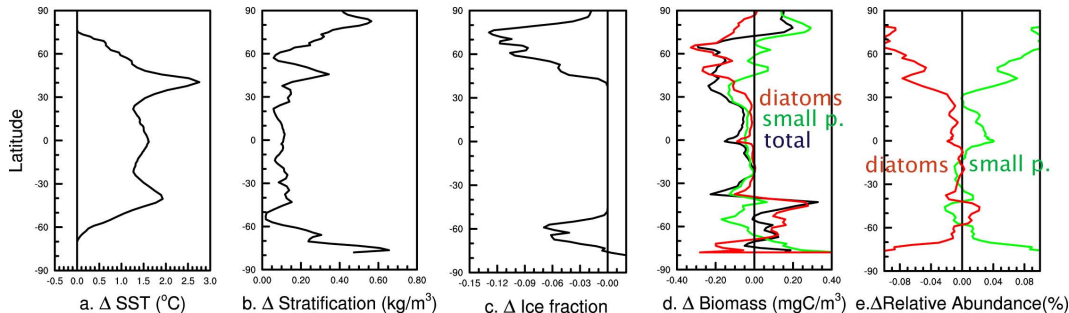
Fig. 3. Zonal mean response to climate change (calculated as difference from years 1980–1999 to 2080–2099) of the: **(a)** sea surface temperature in °C, **(b)** fractional change in sea surface stratification, defined as surface minus $200\,\mathrm{m}$ density $\mathrm{kg/m^3}$, **(c)** the ocean area covered by sea ice at some point in the year in $10^{12}\,\mathrm{m^2}$ per degree, **(d)** total (black), small phytoplankton (green) and diatom (red) biomass ($\mathrm{mg\,C/m^3}$) and **(e)** diatom (red) and small phytoplankton (green) relative abundance (no units).
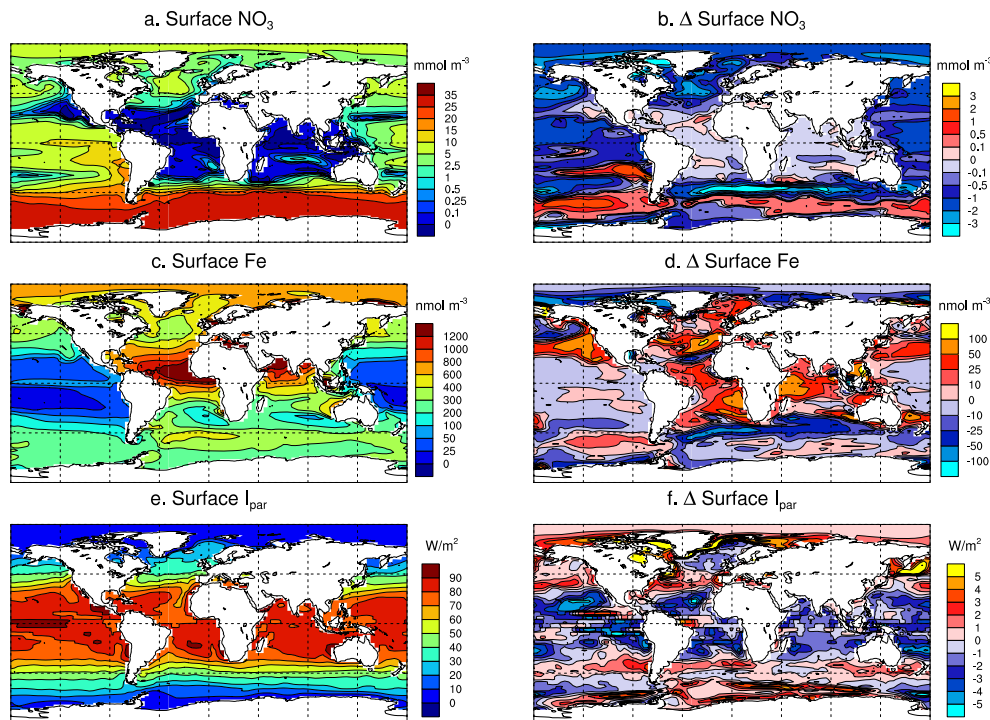
Fig. 4. (**a** and **b**) Surface nitrate in mmol/m³ averaged over 1980–1999 and the change in nitrate between years 1980–1999 and 2080–2099. Same as above for (**c** and **d**) the surface iron in nmol/m³ and (**e** and **f**) surface irradiance I_{par} in W/m². Surface irradiance takes into account the decreasing ice coverage.
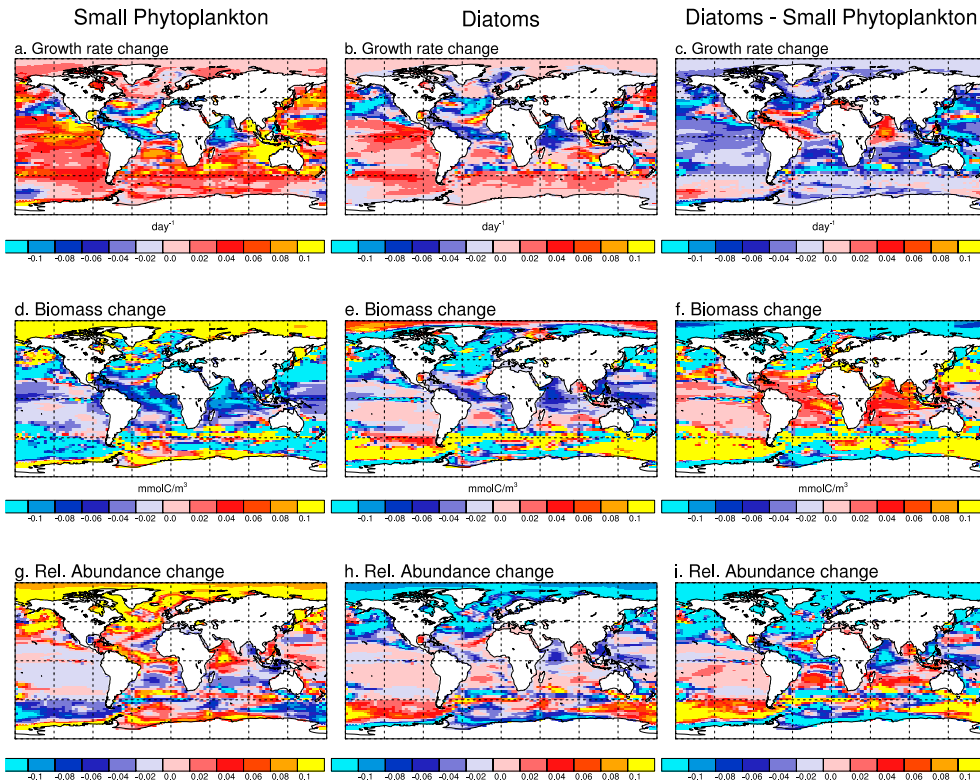
Fig. 5. The 1980–2100 changes in (**a, b, c**) specific growth rate in day-1; (**d, e, f**) biomass in mmol C/m^3; (**g, h, i**) fractional abundance - no units - for small phytoplankton (left panels), diatoms (middle panels), and the difference between diatoms and small phytoplankton (right hand panels). All terms calculated from the respective 1980–2100 linear trends multiplied by 120 years.
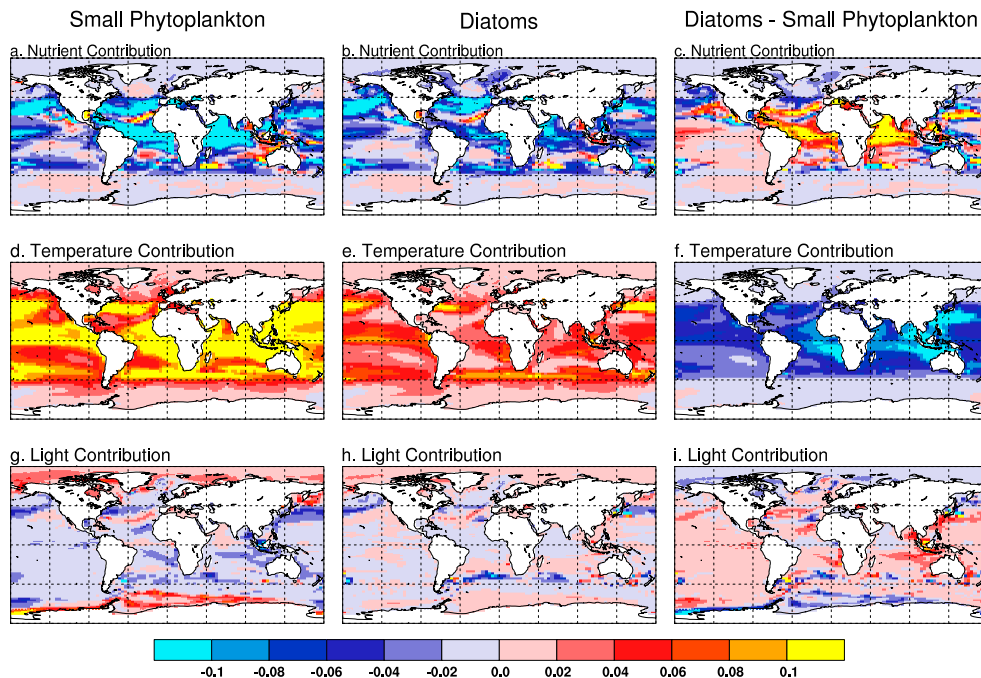
Fig. 6. What drives the 1980 to 2100 change in phytoplankton specific growth rate? Shown are the **(a–c)** nutrient contribution terms $\Delta\mu_x^{nutr}$; **(d–f)** temperature contribution terms $\Delta\mu_x^{temp}$; **(g–i)** light contribution terms to the growth rate trend $\Delta\mu_x^{light}$. All terms calculated from the respective 1980–2100 linear trends multiplied by 120 years, in units of d^{-1}, and shown for small phytoplankton (left panels), diatoms (middle panels), and the difference between diatoms and small phytoplankton (right hand panels).
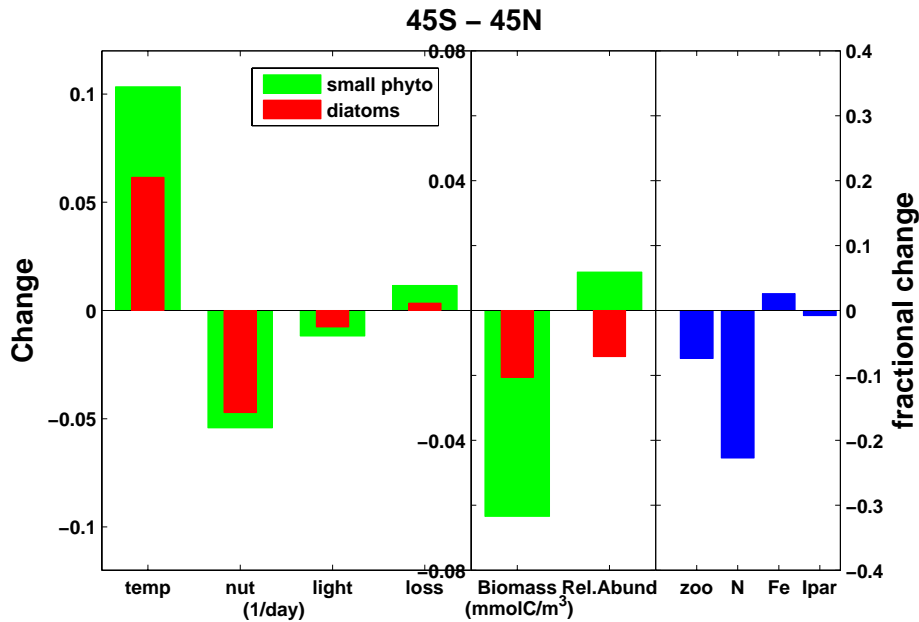
Fig. 7. Climate driven changes in small phytoplankton (green) and diatom (red) growth and loss terms averaged over the 45° S–45° N region. Shown are the temperature, nutrient and light contributions to the change in specific growth rate in units of d^{-1} ($\Delta\mu_x^{temp}$, $\Delta\mu_x^{nutr}$, $\Delta\mu_x^{light}$ calculated from the respective linear trends multiplied by 120 years; diatom or small phytoplankton biomass used as weight in biome averaging); changes in total phytoplankton loss rate (sum of grazing, linear loss, aggregation rate, in d^{-1}); the 1980–2100 linear trends in biomass (mmol C/m^3) and the 1980–2100 change in diatom relative abundance (no units, total biomass used as weight in biome averaging). The fractional changes from 1980–1999 to 2080–2099 in zooplankton carbon, nitrate, iron and total irradiance I_{par} are shown in blue (no units).

Title Page

Abstract | Introduction

Conclusions | References

Tables | Figures

◄◄ | ►►

◄ | ►

Back | Close

Full Screen / Esc

Printer-friendly Version
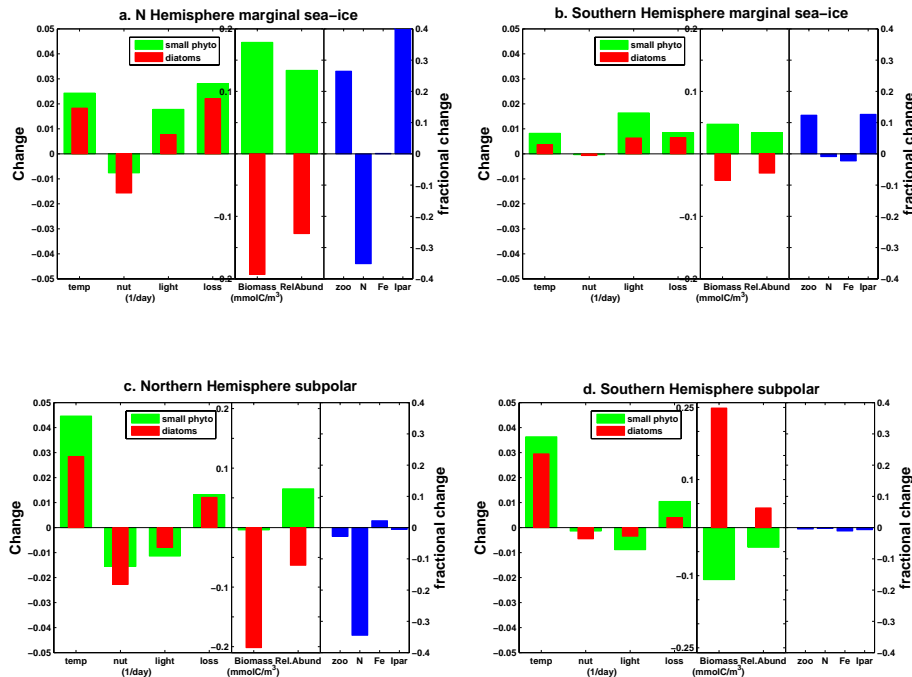
Interactive Discussion

Fig. 8. Climate driven changes in small phytoplankton (green) and diatom (red) growth and loss terms averaged over **(a)** the Northern Hemisphere marginal sea ice biome **(b)** the Southern Ocean marginal sea ice biome **(c)** the Northern Hemisphere subpolar biome **(d)** the Southern Ocean subpolar biome. Same variables as in Fig. 7. Light and temperature impacts on growth are most important in the marginal sea ice biomes and subpolar biomes, respectively.
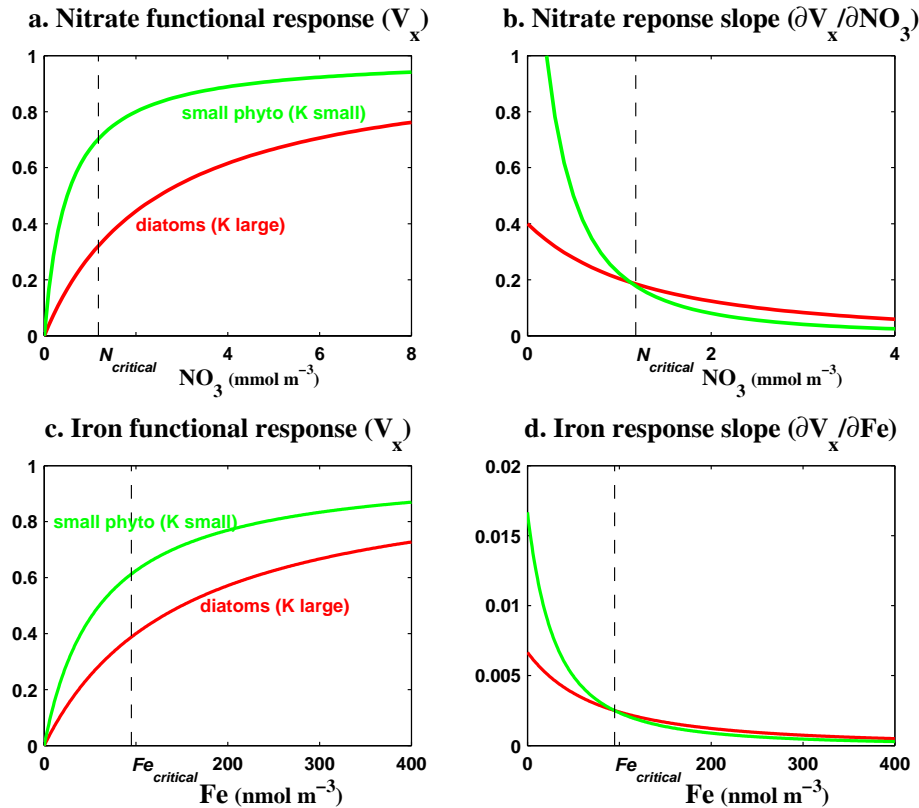
Fig. 9. Illustration of the critical nutrient theory (Sect. 3.2) for nitrate or iron limited regions. For both small phytoplankton (green) and diatoms (red) we show **(a)** nitrate functional response versus nitrate concentration, **(b)** the slope of nitrate functional response, **(c)** iron functional response versus iron concentration and **(d)** the slope of iron functional response. Below the critical nutrient concentration, a change in ambient nutrient impacts more small phytoplankton than diatoms.

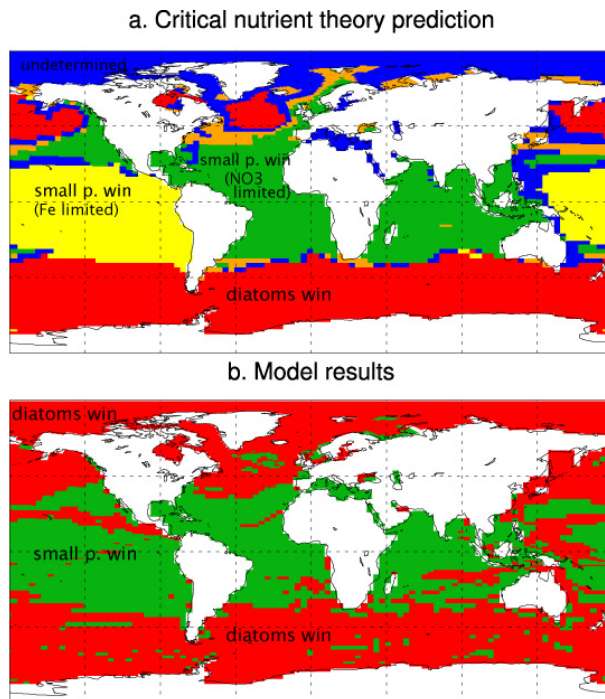a. Critical nutrient theory prediction

b. Model results

Fig. 10. (a) Critical nutrient theory predictions. Green: small phytoplankton expected to win over diatoms in nitrate limited regions; Yellow: small phytoplankton win over diatoms in iron limited regions; Red: diatoms win in iron limited regions; Orange: diatoms win in nitrate limited region; Blue: no theoretical prediction possible, diatoms and small phytoplankton limited by different nutrients. **(b)** Model results. Shows regions where $\Delta\mu_{sp}^{nutr} > \Delta\mu_{diat}^{nutr}$ (green) or $\Delta\mu_{sp}^{nutr} < \Delta\mu_{diat}^{nutr}$ (red). Note that theory predicts well model results; yellow and green areas in (a) coincide nicely with green areas in (b); red and orange areas in (a) coincide with red areas in (b).
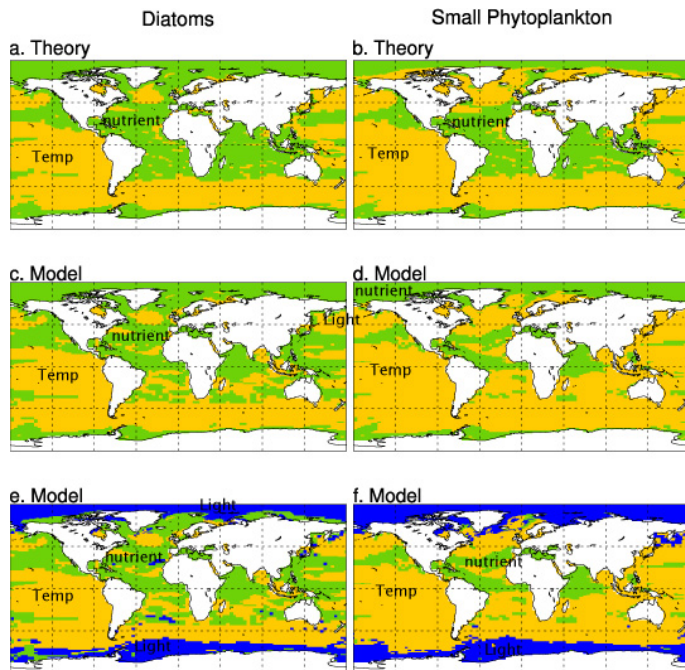
Fig. 11. (**a** and **b**): Theoretical prediction based on Eq. (21) of whether the 1980–2100 growth rate change due to nutrient limitation should be larger than the growth rate change due to temperature. Prediction shown for (a) diatoms and (b) small phytoplankton. Green: growth rate change due to nutrient (either nitrate or iron) dominates; Yellow: growth rate change due to temperature dominates. **(c–f)** Model results. (c and d) Regions where the model calculated 1980–2100 growth rate trend due to nutrient limitation is larger (green) or smaller (yellow) than the growth rate change due to temperature for diatoms (c) and small phytoplankton (d). (e and f) Shows regions where the model calculated 1980–2100 growth rate trend is dominated by either the nutrient limitation term (green), temperature term (yellow) or by the light term (blue).